CSIRO CLIMATE ADAPTATION FLAGSHIP
www.csiro.au

BUSHFIRE DECISION SUPPORT TOOLBOX
RADIANT HEAT FLUX MODELLING

Case Study Three: 2013 Springwood Fire, New South Wales

Glenn Newnham[1,3], Raphaele Blanchi[2,3], Justin Leonard[2,3], Kimberley Opie[1,3], Anders Siggins[1,3]

[1] CSIRO Land and Water

[2] CSIRO Ecosystem Sciences

[3] CSIRO Climate Adaptation Flagship

May, 2014

Report to the Bushfire Cooperative Research Centre

Citation

Glenn Newnham, Raphaele Blanchi, Justin Leonard, Kimberley Opie, Anders Siggins (2014). Bushfire Decision Support Toolbox Radiant Heat Flux Modelling: Case Study Three, 2013 Springwood Fire, New South Wales, CSIRO report to the Bushfire CRC.

Acknowledgements

This project is part of the risk assessment and decision making research programme of the Bushfire Cooperative Research Centre. We gratefully acknowledge all the people who contribute to this research. We would like to thank Fabienne Reisen, Celia Torres-Villanueva from CSIRO, Grahame Douglas from University of Western Sydney and David Boverman from NSW RFS for the careful considerations of this report and the useful comments and suggestions they have provided. We also would like to thank the NSW RFS that have provided the survey and spatial data used in the analysis.

Executive summary

This report is a component of a research program being conducted within the Bushfire Cooperative Research Centre for the development of house and community level Bushfire Decision Support Tools. Specifically, the terms of reference for the projects are to perform a modelling simulation of the final phases of fire approach to case study areas using:

- readily available predictive tools available remotely sensed data (terrain, lidar (for vegetation profiling), house footprints, etc
- existing known and/or simulated (e.g. phoenix) fire isochrones to emulate fire arrival direction and rate of approach
- relate rate of spread to an estimate of available vegetation fuel to estimate flame front dimension
- the flame dimension and rate of spread estimates to estimate the time radiation projection profile as experienced by the houses (using vulnerability assessment tools and methods).
- simple radiation ignition criteria to estimate which houses may have ignited due to radiation and flame exposure from the formal fire front defined above.

This report details the third of three case studies used to explore spatial modelling of RHF incident on a house during a fire as an alternative of the AS3959 approach for hazard classification. This case study uses data collected during and after the fire that occurred at Springwood in NSW in October 2013. The study develops detailed modelling of radiant heat incident on houses using topographic information, while accounting for vegetation (fuel) structural variability across the landscape. Case Study 1 (Siggins et al., 2013) derived fuels information based on airborne lidar data by performing ray tracing through a scene of trees based on simple opaque spheroids. Case Study 2 investigated the feasibility of applying landscape level radiant heat modelling where only coarse fuels information is available (Newnham et al., 2013). This case study again uses airborne lidar data but rather than representing trees as simple spheroids, this case study uses a three dimensional turbid medium approach, where the density of vegetation derived from airborne lidar is directly related to the level of attenuation. In addition to vegetation attenuation, the attenuation of RHF by surrounding building is taken into account.

A total of 216 homes were considered in the case study analysis. Post-fire surveys indicated over 58% of the homes (126) sustained some damage as a result of the fire including 79 houses destroyed and 42% of the houses (90) were untouched. Radiant heat flux modelling indicated that 96 homes (44%) were subjected to 12 kW/m^2 exposure for greater than 30 seconds, suggesting the potential for radiant heat based ignition. Only low levels of statistical separability were shown between damaged and untouched homes based on metrics derived from RHF profiles in this case study. There are a number of factors which we suggest have contributed to this result. Fuel structures across the study area varied less than in past case studies. Most of the homes in case study 3 backed directly onto bushland with small fuel management zones. This led to less variability in RHF profiles, which makes prediction of loss more challenging. The conditions on the day of the fire were also relatively benign when compared to our past case studies. As a result we would suggest that radiant heat played very little direct part in house loss in the fire. The fact that most losses were attributed to ember attack has likely led to a less predictable situation for house loss.

1 Introduction

This project is a component of a broader research program conducted within the Bushfire Cooperative Research Centre for the development of a house and community level Bushfire Decision Support Tools. The project aims to better understand and assess the bushfire impact at the rural-urban interface and is broken into two major components:

- Interface fuel characterisation: This body of work has provided information on combustible elements that contribute to the vulnerability of the interface (Leonard et al., 2011) and,
- Vulnerability assessment and parameterisation: This component aims to better understand the relationship between modelled fire behaviour and vulnerability at the urban interface (Blanchi et al., 2011; Leonard et al., 2012; Siggins et al., 2013; Newnham et al., 2013).

The methods developed have focused on assessing the significance of radiant heat flux (RHF) as an explanatory variable for house damage using historical fire and house loss data. Three case studies have been used to explore the vulnerability of urban interfaces at a community scale.

The first case study focused on the vulnerability assessment of Pine Ridge Road, an area affected by the 2009 Kilmore fire (Siggins et al., 2013). The study used two approaches to assess the RHF, a two-dimensional transect based approach and a three-dimensional ray tracing approach. Both approaches showed promising results in explaining house loss during the fire. Conclusions suggested that the transect based approach did not perform as well as the three-dimensional approach because it did not account for all fuels involved. The three-dimensional approach was preferred but was computationally more intensive and provided an overly simplified structure for vegetation elements (opaque spheroidal crowns).

Case study 2 considered the Wangary fire of 2005 and investigated the feasibility of applying community scale RHF modelling where only coarse fuels information was available. No airborne lidar data was available for the study and fuels information was derived from coarse land cover classification information. This represented a worst case scenario for vegetation information as an input to predictive RHF modelling, since all spatial datasets were low resolution data available at the continental scale. The results of case study 2 showed that despite the low resolution of the input data it was possible to model radiant heat as a flame progresses towards individual houses, taking into consideration variations in fuel load, topography and RHF attenuation between the fire front and the house (Newnham et al., 2013).

This report outlines the third and final case study for the fire that occurred on October 18th 2013 in Springwood NSW. The RHF modelling has been modified to incorporate the best aspects of the two- and three-dimensional lidar based modelling developed in case study 1. The model is applied for 216 houses within the affected region of the Springwood fire and the significance of RHF profiles quantified in terms of their ability to explain damage to houses.

The approach developed for this case study brings together the learning from the previous studies. It takes into account detailed modelling of the vegetation and topography, and includes the estimation of attenuation of RHF by the elements in line-of-sight between the house and the flame front. This case study benefits from the detailed vegetation structural information from lidar data but builds on the methods previously developed (Siggins et al., 2013) for representing this structure within the modelling framework. In addition to previous case studies the attenuation of RHF by surrounding buildings is also taken into account in the model. As in case study 2, exposure of the house has been assessed using metrics derived from the RHF profiles. These describe the maximum RHF exposure (similar to the AS3959 method B approach), the accumulated energy at the houses and the duration of house exposure above a threshold for unpiloted ignition of timber (Newnham et al., 2013).

2 The Springwood Fire

On the 16th of October 2013 a series of fires started in the Great Blue Mountain area under dry hot and windy conditions. The situation worsened on the 17th and 18th of October as strong winds associated with a cold front enhanced fire activity in the Blue Mountains (BOM, 2013a). Two fatalities were associated with the fires, which caused the loss of more than 200 houses. A preliminary house damage assessment done by the NSW RFS is presented in Table 1.

Table 1 Number of houses partially damaged and totally destroyed in the Blue Mountains fires of October 2013 (source: NSW RFS[1])

Fire location	Houses partially damaged	Houses completely destroyed
Hank Street, Port Stephens	6	0
Hall Road, Balmoral	2	2
Rutleys Road, Wyong	3	3
Linksview, Springwood	109	193
State Mine, Lithgow	1	3
Mt York, Mt Victoria	1	7
Total	122	208

The most affected area was in Springwood, 70km west of Sydney in the Blue Mountains. The fire spread over 3500ha (Figure 1 and Figure 2), destroyed 193 houses, and claimed the life of one person. The Springwood fire started close to Linksview Road just before 1:30pm on the 17th of October as a result of powerlines damaged due to strong wind (NSW RFS[2]) and impacted the Winmalee and Yellow Rock areas, north of Springwood.

The study area

A subset region was chosen in the south of the Winmalee area. This was one of the areas most heavily impacted by the fire (Figure 2). Indication of fire arrival was given by a fire emergency warning issued to the Springwood areas on the 17th of October 2013 at 3:45pm[3] (information from thermal line scanner imagery showed that the houses in the study area were well alight at 5:07pm, source NSW RFS). The study area includes urban development along ridge top roads, which are surrounded by dry eucalyptus forest.

[1] New South Wales Rural Fire Service. Update – Damage assessment and fire investigation. Media release, 19 October 2013. (http://www.rfs.nsw.gov.au/file_system/attachments/State08/Attachment_20131019_1D0FD239.pdf). Accessed 01/04/2014

[2] New South Wales Rural Fire Service. Update – Fire investigation. Media release, 19 October 2013. http://www.rfs.nsw.gov.au/file_system/attachments/State08/Attachment_20131019_1E1AEAB1.pdf. Accessed 01/04/2014

[3] The Early Warning Network (http://www.ewn.com.au/alerts/2013-10-17-050300-40620-865.weather, accessed April 2014)

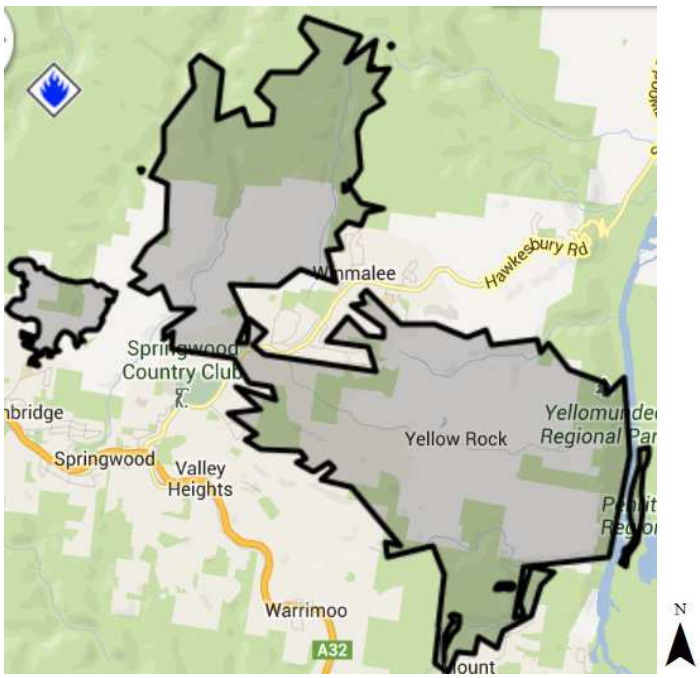

Figure 1 Linksview Road, Springwood (Blue Mountains) fire, final extent of the fire (source: NSW RFS[4])

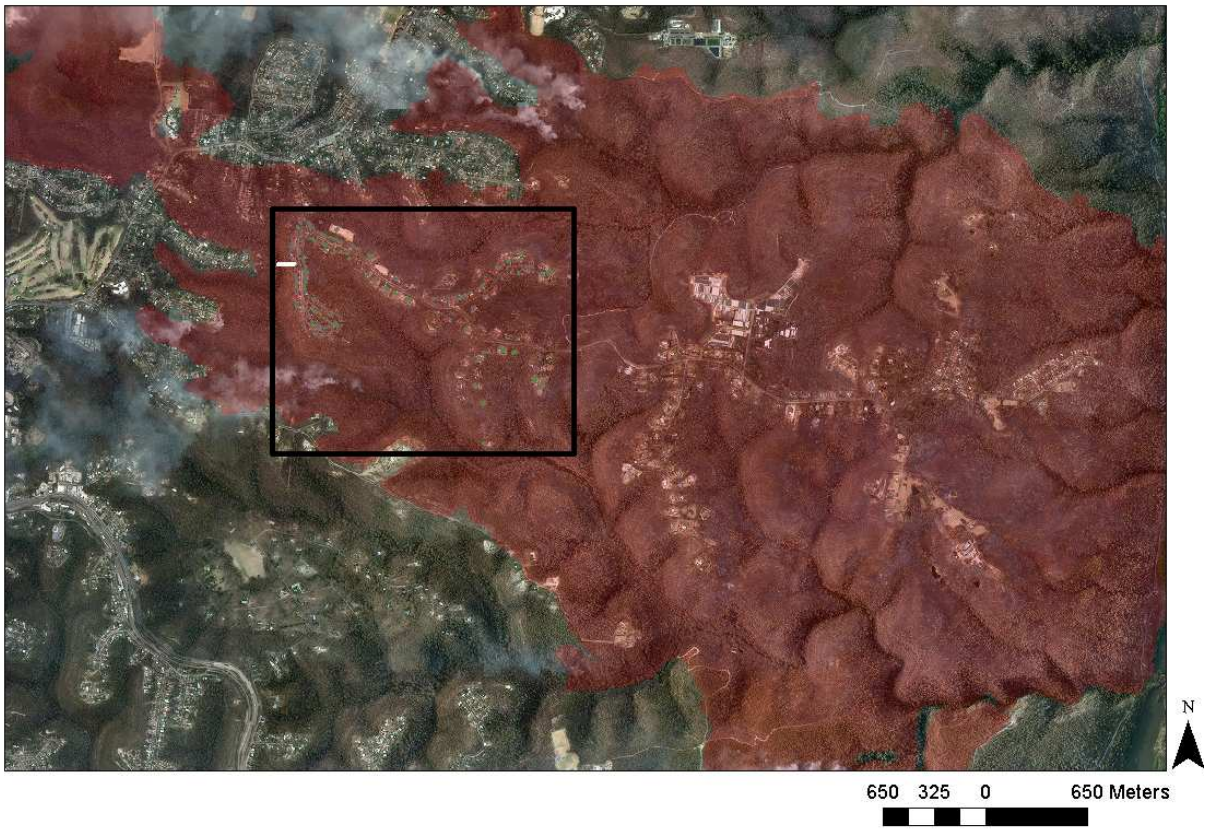

Figure 2 Post bushfire aerial imagery of Springwood study area (in black) and fire extent (in red)

[4] http://www.bluemountains.rfs.nsw.gov.au/dsp_content.cfm?cat_id=4589. Accessed April 2014

Weather conditions

The month of September was the warmest on record in Australia (highest on record in the areas affected by the fire) with below average rainfall in New South Wales and other part of the continent (BOM, 2013b). These conditions associated with northerly winds contributed to an early start of the bushfire season with more than 50 bushfires alight before the 10th of September.

The same conditions persisted in October, with warm weather, temperature above average and rainfall well below average (BOM, 2013a). These dry and hot conditions in conjunction with high wind were responsible for the spread of bushfires in New South Wales from the 10th of October.

The weather conditions on the day of the fire (17th of October) worsened with the arrival of a cold front, which generated strong winds in the Blue Mountains. The synoptic sea level pressure charts for the 16th and 17th of October provides an indication of the progression of the main front across Australia (Figure 3).

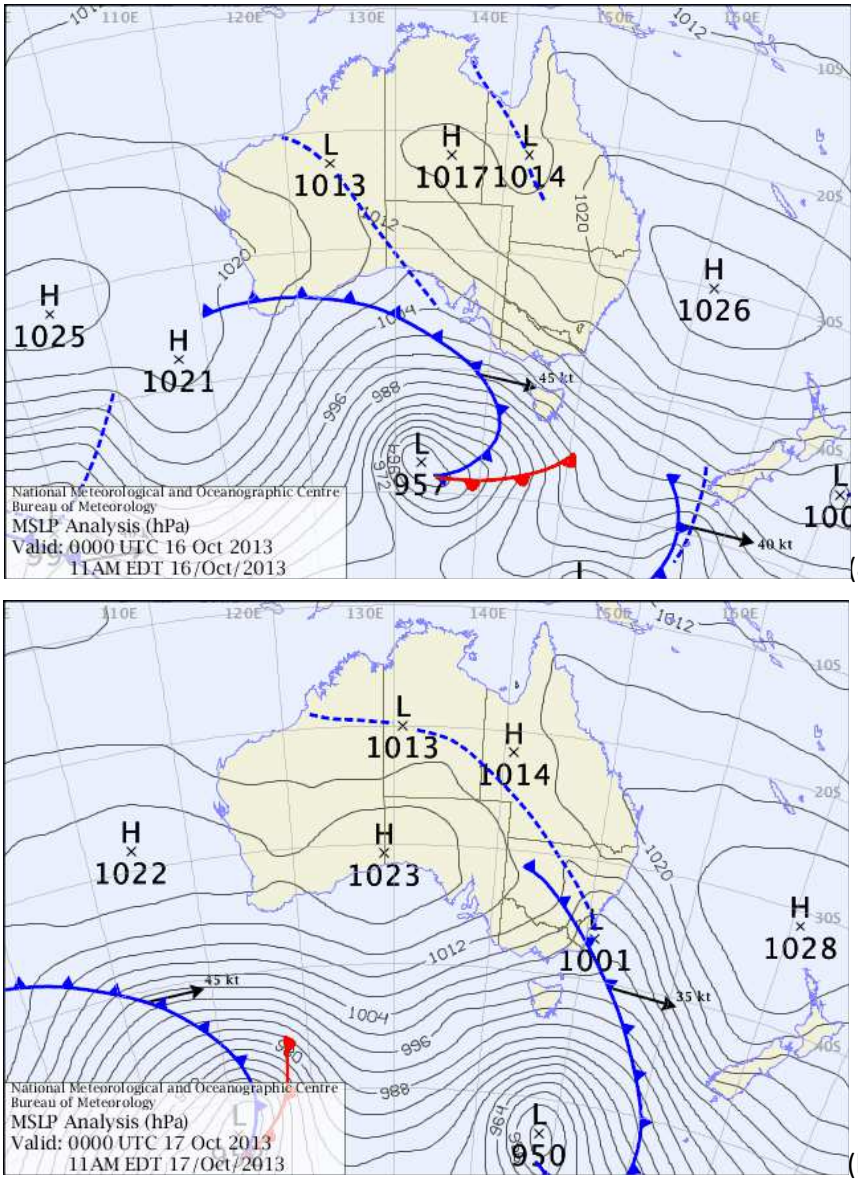

Figure 3 Synoptic atmospheric pressure chart for 11am eastern daylight saving time on the (a) 16th of October 2013 and (b) 17th of October 2013 (source BOM, 2013)

The weather data used for the analysis was recorded at the Springwood automatic weather station (AWS station number 63077), 2 km south from the study area. Only 9am and 3pm records were available from the station. The plot of relative humidity and temperature at 3pm during the month of October is shown in Figure 4.

On the day of the fire (17th of October) the temperature at 3pm was 29.9°C, the relative humidity was 11% and the wind speed was 37 km/h from a north westerly direction. Assuming a drought factor of 10, the Forest Fire Danger Index (FFDI) at 3pm was 55 (using Noble equation, Noble, 1980). This is representative of the weather conditions before the wind changes and might not be representative of the conditions experienced at the time of fire impact on the study area (to note that records of strong wind gusts were associated with the changes, BOM, 2013a).

At an FFDI of 55 the weather conditions are considered severe. However, the high number of losses observed during the fire is higher than expected for Australia at this severity level (Blanchi et al 2010). In the case of the Springwood fire, terrain slope increased the fire severity in the bushland surrounding the houses. In spite of this there was little evidence of direct flame contact or radiation damage on homes. As such, losses were predominantly due to ember attack.

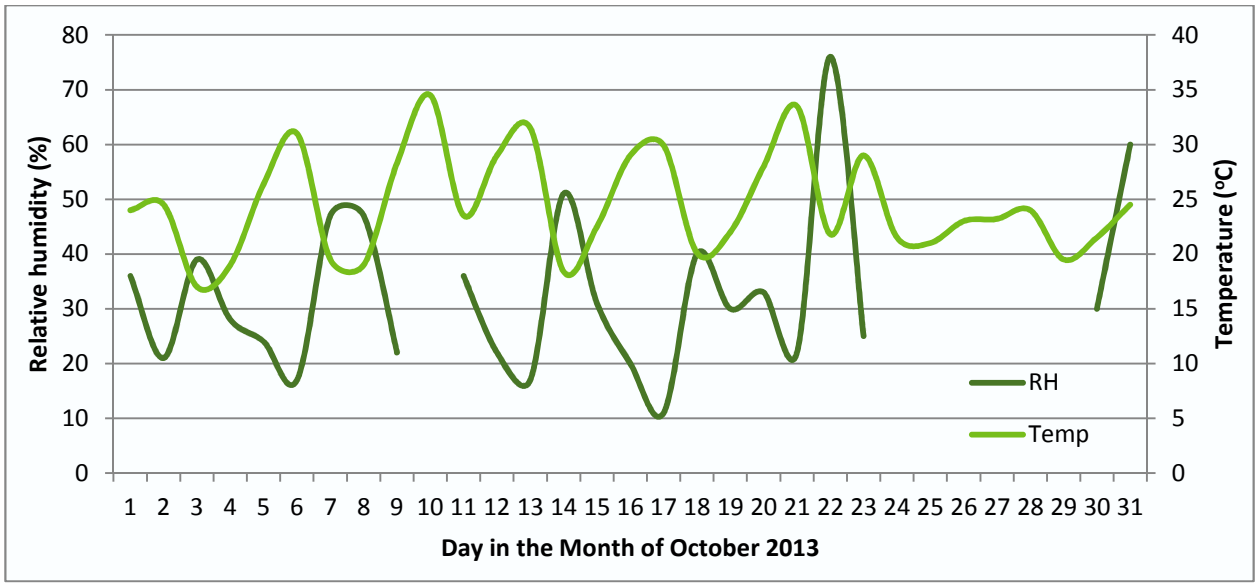

Figure 4: Relative humidity and temperature at Springwood AWS (63077), October 2013. Observation recorded at 3pm on each day in October.

3 Spatial Datasets

Spatial data used in this case study was provided by the NSW Rural Fire Service (RFS) and included airborne lidar data, detailed information regarding the location of houses and building materials collected after the fire. Both topography and vegetation information was derived directly from the airborne lidar data.

3.1 House Locations

A detailed house survey was carried out after the Springwood fire from the 20th of October by a team from the NSW RFS, Fire and Rescue NSW, and CSIRO. The survey was conducted using an Android Tablet based application developed by CSIRO[5]. This captures details of the house and surrounding, such as its design and the surrounding landscape. For each feature different attributes were recorded such as level of damage, along with details of building construction and materials. The survey was carried out on the towns of Winmalee, Lithgow and Mount Victoria which were among those severely affected by the recent bushfires. More than 500 houses were surveyed (including damaged and untouched houses).

For the purpose of analysing the survey data, the study area was divided into two subset areas based on their different urban layout (Table 2 and Figure 5). On the west, study area A includes Buena Vista Road and Singles Ridge Road. Situated on the top of the hill between two state parks, Buena Vista Road presents dense urban development along the road, surrounded by temperate eucalyptus forest (dry sclerophyll forests, shrubby formation[6]). The eastern area of the case study (study area B) includes Long Angle Road and Heather Glen Road. These areas are more recently developed, with scattered houses and some small paddocks, surrounded by temperate eucalyptus forest (dry sclerophyll forests).

In the Springwood case study area 216 houses were surveyed of which 126 houses were damaged and 90 houses were untouched (See Table 2 and Figure 5). A classification of 'Untouched' means that the house was impacted by the bushfire (exists within the final fire extent) but there was no damage sustained. The severity of house damage was collected in the survey and includes five standard categories (e.g. Leonard & Blanchi, 2005; Leonard et al., 2009):

- Superficial - small ignitions that were, in almost all cases, extinguished before they entered the structure, e.g. discoloration, paint blistering, small scorch marks.
- Light damage - some penetration before being extinguished, confined to item first ignited and immediate surroundings, e.g. cracked or broken window, burnt window frame.
- Medium damage - combustion that has spread to secondary elements, or extensive radiation impact, e.g. flame spread involving a large area of the facade, flame entry into the building or building cavity.
- Heavy damage - flames have entered the house and engulfed at least one room in the house, or sufficient external combustion to compromise the structural integrity of the house.
- Destroyed - total structure loss. House is typically rendered un-occupiable.

[5] https://blogs.csiro.au/climate-response/stories/new-apps-for-critical-bushfire-assessment/). Accessed April 2014
[6] Vegetation map (source: NSW RFS)

The percentage of houses that were damaged in the study area (58%) is comparable to the percentage observed in the Victorian fires in 2009 (54%) (Leonard et al., 2009). All the houses within the study area were surveyed irrespective of their perceived damage status.

House footprints and associated thematic data collected during the survey were used for determining the house location as a focal point for RHF exposure analysis. In this study three variables associated with each house have been considered: the degree of damage to the house, the mechanisms of bushfire attack and the role of surrounding vegetation on house damage.

Table 2 Number of houses damaged and untouched in the two areas of the Springwood study area- indicative house density in those two areas is also shown. Note that the study area is a subset of the Linksview-Springwood fire described in Table 1

Area	Area (ha)	Total number of houses	House density (no./ha)	Houses damaged	Houses untouched	Percentage of damaged houses
Study Area A (Buena Vista Road on the west side and Singles Ridge Road)	55.8	142	2.5	81	61	57%
Study Area B (East of Singles Ridge Road, Long Angle Road and Heather Glen Road)	190.2	74	0.4	45	29	61%
Total Study area	246	216	0.9	126	90	58%

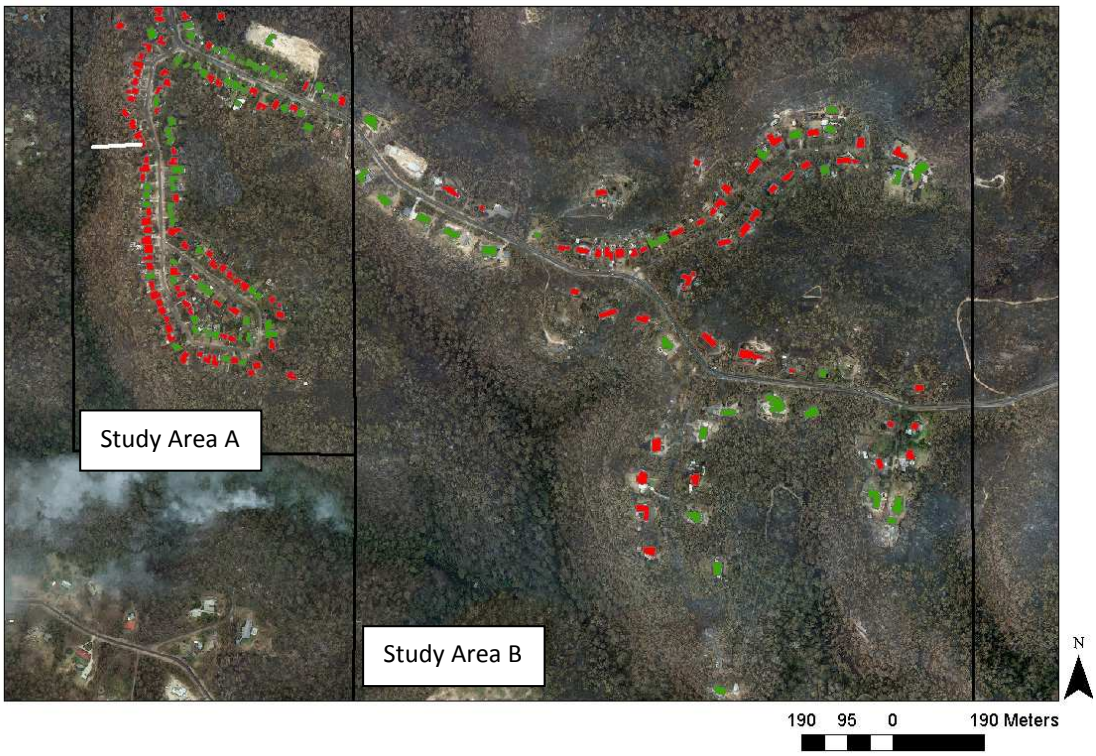

Figure 5: Post bushfire aerial true colour imagery showing houses surveyed in the Springwood case study area - destroyed houses are shown in red and untouched houses in green.

The fire intensity observed in true colour aerial imagery varied across the study area. In some areas the trees were scorched with isolated cases of tree crown defoliation. These more severely burnt areas tended not to be very localised and adjacent to house assets (Figure 5). According to the post bushfire survey the fire spread was best characterised as a surface fire spread, with mainly surface fuel involvement.

3.2 Topography

The study area is hilly terrain, with elevations ranging from 150m in the valleys to 328m on top of the ridges. All houses in the study area were located along ridge lines and surrounded by narrow gullies (Figure 6). Terrain would have played a significant role in the fire behaviour, with slopes increasing the fire rate of spread. Luke and McArthur (1978) experimental work indicated that the rate of spread doubles on a 10^{o} slope and could increase almost fourfold on a 20^{o} slope. In addition, narrow valleys can act as a channel for the wind and increase the fire spread (Viegas & Simeoni, 2011).

The lidar data was collected in February 2011 using a Leica ALS50-II instrument. The flying height was 2199m and the average point density for the area was 1.65 pulses per square meter. The data was provided in the lidar interchange format (LAS) with four tiles covering the study area. A Digital Elevation Model (DEM) at 1m resolution was derived from the lidar data and was provided directly by the airborne data provider.

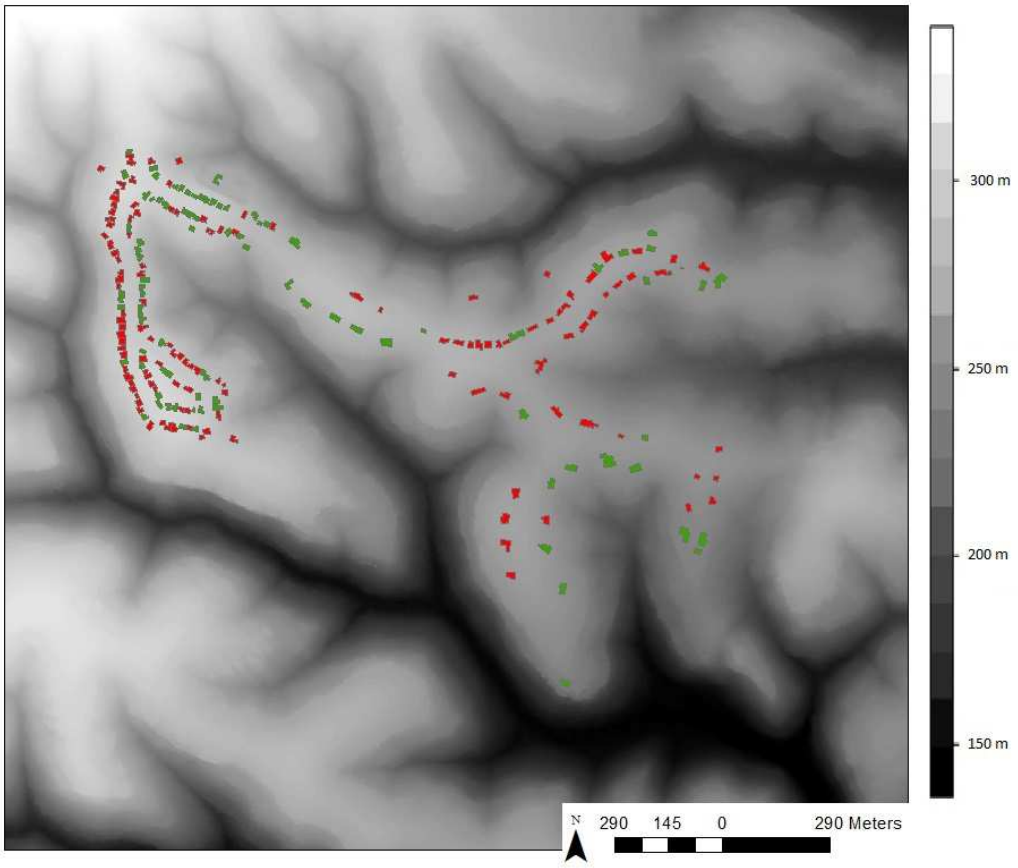

Figure 6: Digital elevation model for the Springwood study area based on airborne lidar data. Destroyed houses are shown in red and untouched houses are shown in green.

Fire spread direction can be used to assess the specific fuels and topography that influenced the fire as it impacted a specific home or out-building. Very little information was available on fire spread and fire direction for the Springwood region. Thermal line scanner imagery showed that at 5:07pm on the 17th of October the complete study area was alight (Figure 7). In the absence of clear empirical fire spread information, anecdotal accounts of the fire spreading from valleys up onto the ridges was used as the primary source of information for modelling fire direction (source NSW RFS). These fire directions were determined using topographic aspect around each house (Figure 8).

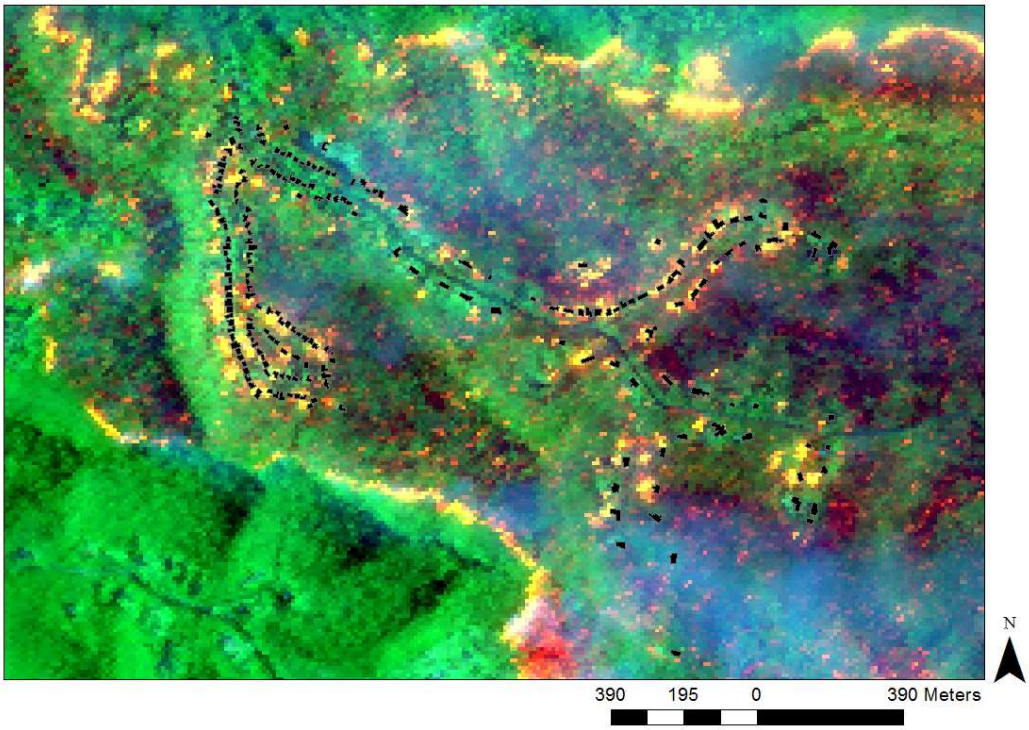

Figure 7 Thermal line scanner imagery of the study area at 5:07pm on the 17th of October 2013. Houses impacted by the fire within the study area are shown in black.

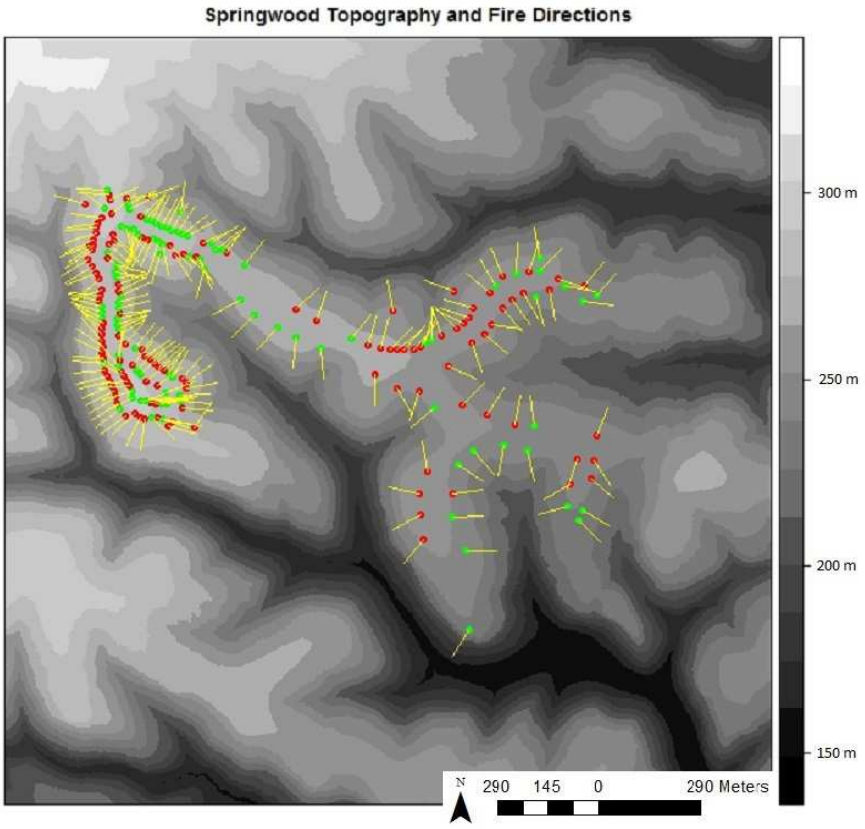

Figure 8 Springwood topographic elevation (in meter) and fire approach directions for each house shown as yellow lines. House locations shown in red were damaged by the fire and house locations shown in green were surveyed as untouched.

3.3 Fuel Load and Vegetation Height

Information on vegetation (height and fuel load) was obtained from the lidar data. For each house within the study area, a series of transects were interrogated covering the angular range 90 degrees either side of the fire approach direction. A total of nineteen transects were used for each house, each separated in azimuth by 10 degree and stretching out to 100m from the face of the house. Along each transect, lidar points were extracted and the vegetation fractional cover and height were determined at 1m intervals. The presence of other houses along the transect was also determined, based on the house polygons collected during the post fire survey.

At each 1m step along the transect the fractional cover was determined, based on a lidar derived cover fraction (the complement of lidar gap probability). The maximum cover fraction for the study region was associated with the fuel load specified for forests in AS3959. Canopy top height was also determined from the lidar data, as the height of the maximum lidar point. As no independent fuel load assessments were available, no quantitative validation of the fuel load and fuel heights was performed. A more detailed description of the procedure for deriving fuel characteristics and their impact of RHF is discussed in the following section.

4 Methods

4.1 Flame Intensity and Height

The fire intensity and flame height were derived from the equations specified in AS3959 (McArthur, 1973, 1967; Noble et al., 1980). These are the same equations used for case study 1 and case study 2 (Siggins et al., 2013; Newnham et al., 2013). For case study 3, fuels were characterised using a series of 100m transects distributed evenly in azimuth and spanning 90 degrees either side of the fire approach direction. Each transect is sampled at 1m intervals to determine the appropriate fuel load and terrain attributes for rate of spread and fire line intensity calculations. The rate of spread R was determined using McArthur Mark V forest fire danger model (1973) as specified by Noble (1980):

$$R = 0.0012 \times FFDI \times w \quad (1)$$

where $FFDI$ is the MacArthur Forest Fire Danger Index (McArthur, 1973) and w is the surface fuel load. We have used the $FFDI$ of 55 calculated for 3pm on the day of the fire (see section 2).The surface fuel load was determined from the level of overstorey cover derived from lidar data. As the main vegetation type in the area is open forest, a maximum surface fuel load of 25t/ha was used (Standards Australia, 2009). Only surface fuel load was considered as evidence collected on the day showed no canopy involvement in the fire (see section 3.1). Slope correction was employed to the fire rate of spread based on 10m weighted moving average filtering of the DEM data along each 100m transect. A maximum of 30 degrees of correction was assumed as specified in AS-3959 method B (2009). The correction for slope expressed in degrees (θ) is specified by Noble et al. (Noble et al., 1980) as:

$$\mathrm{R_{slope}} = \mathrm{R} \times \mathrm{e}^{0.069 \times \theta} \quad (2)$$

where θ is positive for an upward slope approaching the house and zero for a downward slope. Based on this corrected rate of spread and the surface fuel load (w) in t/ha, we calculate the fire intensity (I) in kW/m^2 using the AS3959 approach (Byram, 1959) as follows:

$$\mathrm{I} = \frac{\mathrm{H} \times \mathrm{w} \times \mathrm{R_{slope}}}{36} \quad (3)$$

where H is the heat of combustion (~ 18600KJ.Kg^{-1}).

Flame length (L_f) is critical in the calculation of the view factor, particularly where vegetation attenuation may play some part in reducing exposure. Any flame below the vegetation height is attenuated by vegetation along the line of sight to the house, while flame that protrudes from the top of the canopy may experience no attenuation (unless it re-enters the canopy due to an increased canopy height or topographic variation). The forest flame length equation as specified by Nobel (1980) is thought to overestimate flame length. For this reason, a slightly modified equation is employed in AS3959 (Standards Australia, 2009). However, this equation is not detailed in the scientific literature, so we have adopted the citable equation for our modelling. This estimation of L_f for forests is based on Noble et al. (1980) as follows:

$$L_f = \left((13 \times R_{slope}) + (0.24 \times W)\right) - 2 \quad (4)$$

This view factor for a given flame length is modified by the flame angle. The approach taken by AS3959 (2009) is to use the worst case scenario, which is effectively a flame angle such that the view direction is normal to the flame surface. This is determined iteratively in AS3959 but is calculated arithmetically in this work as specified in Newnham et al. (2013).

4.2 Calculation of View Factor

The view factor used in the case study 3 is similar to the one developed for case study 2. From the perspective of a point on a house or other asset that may be exposed to radiant heat, the proportion of the hemisphere in the direction of the fire front that flame can be observed is known as the view factor (Drysdale, 1985; Sullivan, 2003; Zárate et al., 2008). AS3959 specifies a fire front width of 100m, unless the width of classified vegetation justifies the use of a lesser value (Standards Australia, 2009). The azimuthal angular span for this 100m flame front ($\Delta\varphi_f$) is dependent on the horizontal range from a house (r) and the height difference between the receiver and the flame base $h(r)$. This angular span is given by:

$$\Delta\varphi_f = 2\tan^{-1}\left(\frac{50}{\sqrt{r^2+h(r)^2}}\right) \quad (5)$$

where $h(r)$ is the height of the terrain at distance r in the direction from which the fire is approaching relative to the view point on the house. The total view factor (ignoring any topographic or vegetation attenuation) can then be calculated based on the proportion of the hemispherical view (2π steradian) from which radiant heat is emanating:

$$\emptyset = \frac{\int_0^{\Delta\varphi_f}\int_\theta^{\theta+\Delta\theta}\sin\theta}{2\pi}\,d\theta d\varphi \quad (6)$$

$$\theta = \frac{\pi}{2} + tan^{-1}\frac{h(r)}{r}$$

$$\Delta\theta = 2\,sin^{-1}\frac{L_f}{2\sqrt{r^2+h(r)^2}}$$

where θ is the zenith angle to the base of the flame and $\Delta\theta$ is the angular height of the flame with the face of the flame front normal to the viewing vector resulting in a worst case flame angle for RHF exposure. This integral can be approximated as a trapezium:

$$\emptyset(r) = \frac{\Delta\varphi_f[\cos\theta - \cos(\theta+\Delta\theta)]}{2\pi} \quad (7)$$

4.3 Attenuation by vegetation, topography and building

The view factor shown in Eq.7 does not account for attenuation by any object that might block the field of view between the house and the fire front. The case studies 1 (Siggins et al., 2013) and 2 (Newnham et al., 2013) showed how attenuation (α) by vegetation and topography could be incorporated into the view

factor calculation. In case study 3 this was extended to also incorporate attenuation by buildings other than the modelled RHF receiver object.

For each azimuth transect within $\Delta\varphi_f$, attenuation is calculated at 1m intervals for each zenith angle between θ and $\theta+\Delta\theta$. For areas below the DEM surface and below lidar points that are within any building footprint, $\alpha = 1$. Vegetation attenuation is determined using gap probability (P_{gap}) derived from the number of lidar points intercepted within the zenith angle and range increment. Specifically, P_{gap} (the complement of the cover fraction *C*) from the top of the canopy down to the range and zenith increment is estimated by:

$$\mathrm{P_{gap}}(\theta, \mathrm{r}) = \ 1 - \mathrm{C}(\theta, \mathrm{r}) = \frac{\#\mathrm{z}|\mathrm{z} > r \sin\theta}{\mathrm{N}} \tag{8}$$

where *N* is the number of lidar points within the range increment along the transect and #z is the number of points that fall above the line of sight at zenith angle θ. At any given range *r* this is equivalent to a height above the observer position of *r* sin θ. Assuming a random projection function for vegetation elements (Ross, 1981), the plant area index (PAI) is then given by:

$$\mathrm{PAI}(\mathrm{z}) = \ -2\ln(\mathrm{P_{gap}}) \tag{9}$$

and the plant area density (*PAD*) is then the derivative:

$$\mathrm{PAD} = \frac{\partial \mathrm{LAI}}{\partial \mathrm{z}} \tag{10}$$

attenuation by vegetation α over an increment in range along the line of sight is given by:

$$\alpha = \frac{(1-\mathrm{e}^{-\mathrm{PAD}})}{\sin\theta}\Delta\mathrm{r} \tag{11}$$

The view factor at zenith angle θ and horizontal range *r* can now be computed as the product of the complement of all attenuation coefficients encountered along the line of sight between the house and the flame front:

$$\emptyset(\mathrm{r}, \theta) = \prod_{\mathrm{x}=0}^{\mathrm{x}=\mathrm{r}} 1 - \propto_{\mathrm{x}} \tag{12}$$

If the line of sight encounters the ground surface of a building $\alpha = 1$ and $\emptyset(r,\theta) = 0$. By combining the integral of Eq.12 across the flame front with Eq.6, the view factor for the flame at range r becomes:

$$\emptyset(\mathrm{r}) = \frac{\int_0^{\Delta\varphi_\mathrm{f}} \int_\theta^{\theta+\Delta\theta} [\prod_{\mathrm{x}=0}^{\mathrm{x}=\mathrm{r}} 1-\propto_{\mathrm{x}}] \sin\theta}{2\pi} \mathrm{d}\theta\mathrm{d}\varphi_\mathrm{f} \tag{13}$$

4.4 Radiant Heat Flux

The calculation of radiant heat flux is discussed by Sullivan et al. (Sullivan et al., 2003) and used in case study 1 and case study 2 (Newnham et al., 2013; Siggins et al., 2013). This is based on the Stefan–Boltzmann law and describes the level of RHF incident on a house from a flame front at horizontal range r as follows:

$$\mathrm{RHF(r)} = \emptyset(\mathrm{r})\ \varepsilon\ \sigma\ \mathrm{T}^4 \qquad (14)$$

where the RHF is given in units of kW.m^{-2}, ε is the emissivity for vegetation (assumed to be 0.95), σ is the Stefan-Boltzmann constant (5.67x10^{-11} kW.m^{-2}.K^{-4}), T is the flame temperature (assumed to be 1200K as used in Siggins et al., 2013). Conjecture remains over the correct temperature to use for a forest fire (Sullivan et al., 2003). In this study we have used both temperature of 1090K and 1200K (Standards Australia, 2009; Sullivan et al., 2003). Sullivan highlights the fact that flame size has an influence on flame temperature. Given the relatively small flame lengths experience in this fire it was also considered useful to perform the radiation analysis on the cooler flame temperature of 1090K used in AS3959 (2009) for comparative purposes.

RHF profiles were generated for each house surveyed in the case study. A number of summary statistics based on these RHF profiles are assessed in the results section. These include the time required for the flame front to travel the final 100m towards each house (Time100m), the maximum level of RHF exposure (RHFmax), the total accumulated energy that each house was exposed to (E) and the total period of exposure to a RHF greater than 12 kW/m^2 (Tgt12). This final statistic is based on a reported minimum threshold for ignition of timber building materials (Tran et al., 1992).

5 Results

This section includes the results from the houses survey including the main mechanisms of attack and the surrounding vegetation (the presence of overhanging trees) and the results of modelled RHF for all the houses in the survey with a flame temperature of 1200K and a flame temperature of 1090 K (as specified in AS3959, Standards Australia, 2009). Two examples of individual houses are also presented to discuss in detail the RHF analysis performed on 2 different houses,

5.1 Houses Surveyed

A total of 216 homes were surveyed in the Buena Vista Road area. These homes were impacted by the fire before 17:00pmon the 17th of October 2013 (Figure 7). Over 58% of the homes (126) sustained some damage as a result of the fire.

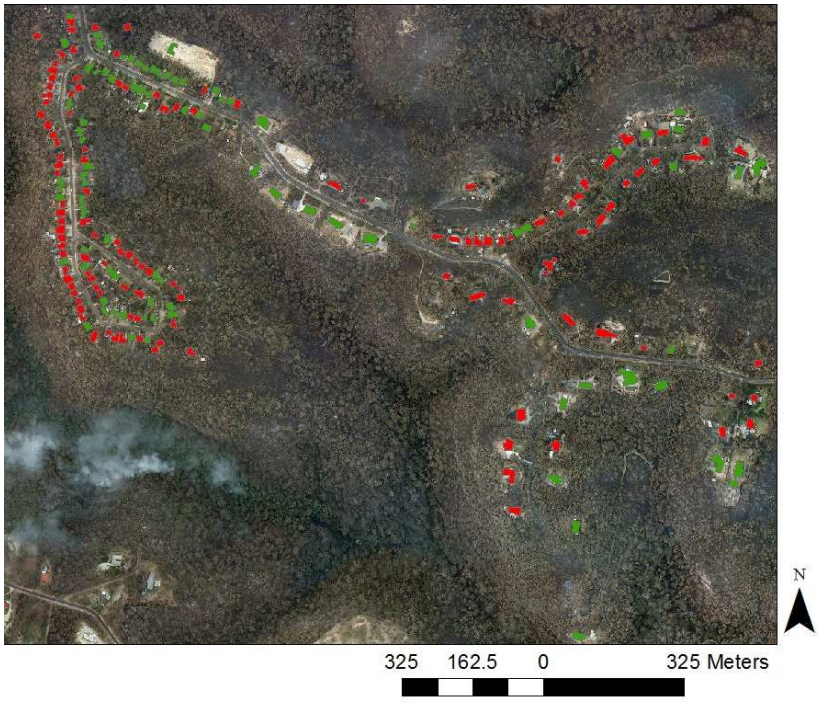

Figure 9: Distribution of damaged (red) and untouched (green) homes within the study area.

Damaged homes were distributed across the study area, but a greater proportion of damage occurred along Buena Vista Road and Heather Glen Road. The loop at the southern end of Buena Vista Road included 21 homes, separating these homes from unmanaged bushland. However, this did not appear to offer significant protection with 10 sustaining damage. All other homes in the study area backed directly onto unmanaged bushland with varying degrees of clearing being apparent.

Table 3 gives a breakdown of the degree of house damage of surveyed structures for the study area and for the Victorian fires in 2009 as a comparison. The percentage of houses that were completely destroyed in the Springwood study area was quite high and comparable to the proportion of houses destroyed in the Victorian fires 2009 (39%).

Table 3 Degree of damage of houses surveyed in study area (Winmalee) and in the Victorian fires 2009 (Leonard et al 2009, Teague et al, 2010)

	Untouched	Superficial	Light Damage	Heavy Damage	Medium Damage	Destroyed	Total
Study area*	90	24	20	1	2	79	216
%	42%	11%	9%	0%	1%	37%	100%
Kilmore East fire**	1766	NA	530	NA	NA	1244	3540
%	50%	NA	15%	NA	NA	35%	100%
Murrindindi fire**	400	NA	74	NA	NA	590	1064
%	38%	NA	7%	NA	NA	55%	100%
Total Victorian fires**	2593	NA	832	NA	NA	2118	5543
%	48%	NA	15%	NA	NA	39%	100%

*Most of the houses in the study area have been surveyed (except 4 houses that have not been surveyed)

** Includes an estimation of all the houses within the fire perimeter

The main mechanisms of bushfire attack (ember, radiant heat and flame contact) were recorded in the survey. Table 4 summarises the proportion of main mechanisms of attack identified for the study area. Ember attack with some radiant heat from surrounding vegetation or other structural fuel (34%) and ember only (14%) were the predominant mechanisms identified in the survey. However the determinations of the main mechanism of bushfire attack are often difficult to assess and require significant training to be able to identify the clues that identify the presence and absence of these mechanisms. This could explain the large proportion of unknown answer (44%) in the survey.

Table 4 Main bushfire mechanisms recorded in the post bushfire survey

	Nb of houses	%
Embers and some radiant heat	74	34%
Embers only	31	14%
Predominantly radiant heat	9	4%
Flame contact from bush vegetation	6	3%
Other	NA	NA
No direct bushfire attack	NA	NA
Unknown	96	44%
Total	216	100%

The presence of adjacent vegetation and overhanging trees has been shown to increase the house loss likelihood (Wilson et al., 1984; Ramsay McArthur, N.A. Dowling, V.P., 1987; Leonard & Blanchi, 2005; Leonard et al., 2009). The post bushfire survey after the Victorian fires 2009 showed a strong correlation between the observation of overhanging trees and house loss (Leonard et al., 2009). Both trees overhanging and/or against the house correlated with house destruction suggesting that these are a significant risk indicator or exposure element for the house. Another possible factor may be the way overhanging trees contribute to the deposition of fine debris around, under and on top of the house. The analysis of overhanging trees in the survey area (Table 5) shows a larger proportion of houses damaged with the presence of overhanging trees (56%) compared to the proportion of houses untouched (19%).

Table 5 Overhanging tree and house damage

	Nb of damaged houses	%	Nb of untouched houses	%
No overhanging trees	19	15%	33	37%
Small proportion of overhanging trees	37	29%	40	44%
Presence of overhanging trees	70	56%	17	19%
Total Nb of houses	126	100%	90	100%

5.2 Individual RHF Cases

Details from two houses discussed below illustrate individual cases for the impact of the Springwood fire. They also show how the input spatial datasets were integrated to develop a profile of RHF exposure. The first case shows the impact on modelled fire behaviour given significant clearing around the house. The second case illustrates the behaviour of the same fire when a house is positioned within significant levels of unmanaged forest fuels.

HOUSE 40

A classic example of well managed vegetation around a home is shown in Figure 10 (post-fire survey reference 40). The house in the south east of the study area has a 23m cleared buffer in the fire approach direction. Post-fire surveys indicated that this house sustained damage. However damage was actually sustained by outbuildings rather than the main residence.

In the RHF model, lidar points were extracted along multiple transects spanning 180 degrees in azimuth and centred on the fire approach direction. Transects for each azimuth contribute to the total view factor used to calculate the RHF profile. Topography, fuel structure and fuel load along each transect are determined using points extracted from the airborne lidar dataset. A single transect in the fire approach direction at house 40 is shown in Figure 11. The 23m managed fuel zone can be seen clearly in the lidar data. Outside this managed zone, the lidar points show an even vertical distribution of fuels out to the 100m extent of the transect.

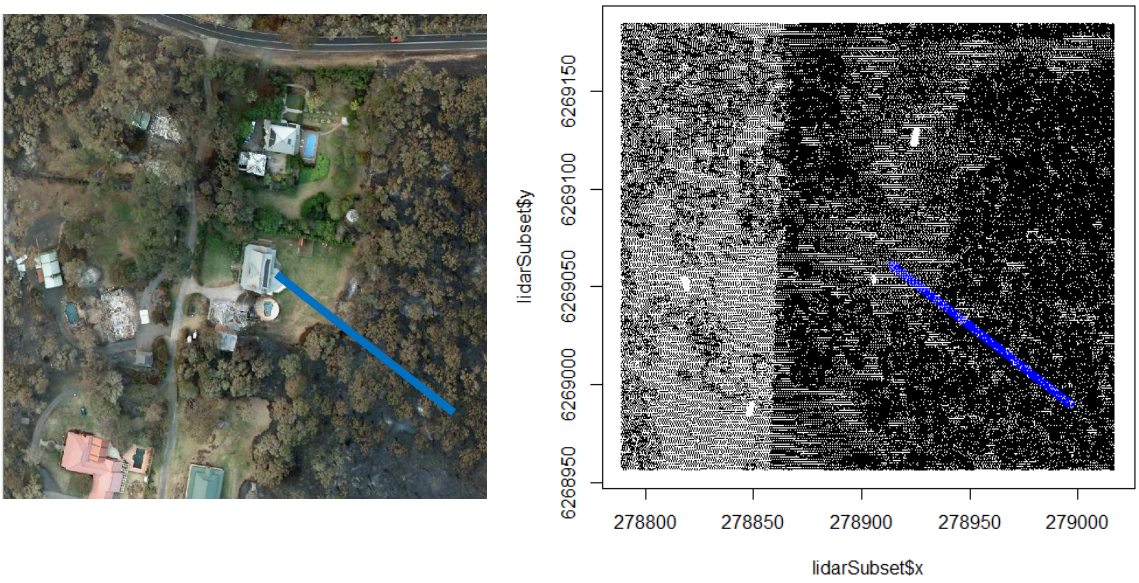

Figure 10: House 40 has a well managed buffer zone between the house and unmanaged forest shown in (left) true colour aerial imagery and (right) the lidar point cloud shown from above with the fire approach direction shown in blue.

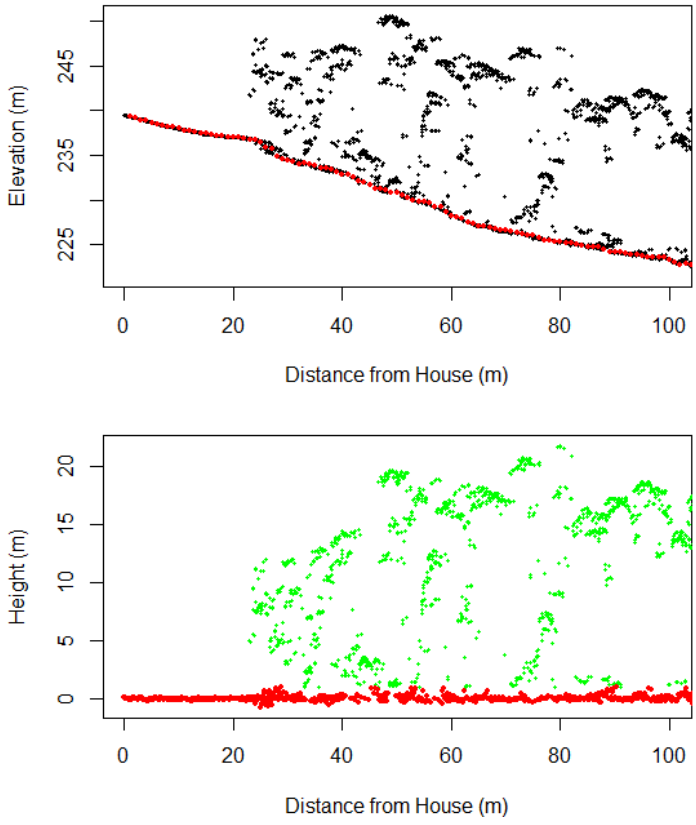

Figure 11: Lidar points extracted along the transect from house 40 in the fire approach direction: (top) indicates the elevation of each lidar point in black and the level of the raster DEM in red; (bottom) shows the lidar points with terrain height removed in order to determine fuel heights; points have been classified as ground (red) or vegetation fuel (green).

The DEM produced by the lidar data provider was used to classify lidar points as vegetation or the ground surface (Figure 11). Due to topographic variation there is an uncertainty regarding points near the DEM surface. These points may be near surface fuels or reflections from bare soil surface. This is an inescapable limitation of lidar data and assumed relationships between elevated fuels and surface fuels are required. Although some evidence for relationships between overstorey cover fraction and the accumulation of surface fuels exists (Walker, 1981), more work is required in this area to properly characterise the relationship specifically for lidar derived cover estimates in order to fully exploit lidar fuel mapping.

Fuel loads in this model were determined based on assumed maxima in PAI and fuel load. We take a value of 9 as the maximum LAI possible for forest vegetation (Asner, 2003) and 25t/ha as the maximum surface load for forest fuels. Thus surface fuel is given by:

$$w = \frac{25 \times PAI}{9} \tag{15}$$

The fuel load derived for house 40 is shown in Figure 12, the derived fire behaviour parameters such as rate of spread, flame height and fire intensity closely follow the form of the fuel load.

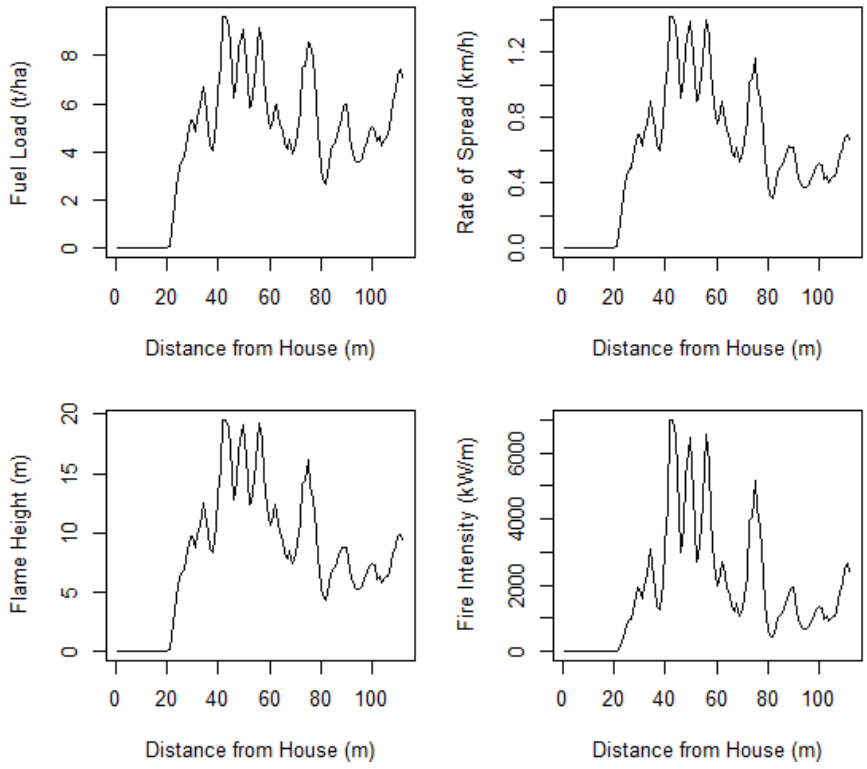

Figure 12: Transects in the fire direction from house 40 of (top left) fuel load, (top right) slope corrected fire rate of spread (bottom left) modelled flame height and (bottom right) fire line intensity.

Lidar data is not only used to determine the fuel load but also the impact of RHF attenuation by vegetation that may exist between the flame front and the house. Attenuation is the complement of transmittance, which is determined based on foliage profile calculations described in the previous section. Elementary transmittance (1-α) describes the proportion of RHF that is transmitted along a unit path length. This elementary transmittance is zero below the ground surface and one above the canopy. At points within the canopy where some interception of RHF occurs the transmittance is dependent on the number of lidar points intercepted within this region and may vary between zero and one.

Transmittance through the vegetation is shown in Figure 13a. Below the horizon (negative elevation angles) the line of sight quickly intersects the ground surface and transmittance becomes zero. Just above the ground surface, some attenuation by vegetation is apparent. In Figure 13b, the cumulative effect of vegetation transmittance becomes more obvious along the line of sight near the ground surface.

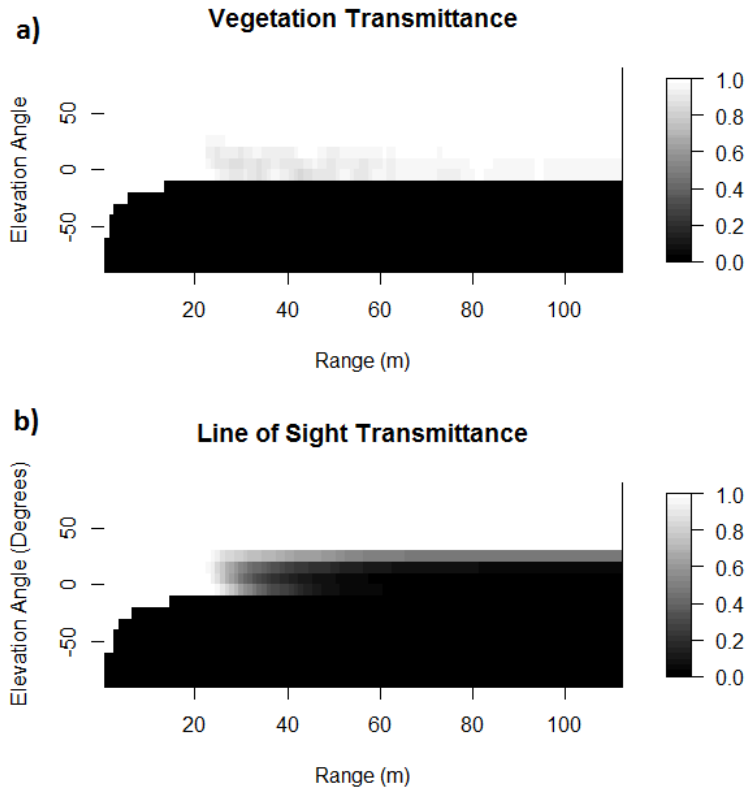

Figure 13: Transmittance out to 100m along lines of sight at different elevation angles from 90 degrees below the horizon to 90 degrees above the horizon: a) the transmittance for an elemental region within the canopy, b) the transmittance out to a given range along the lines of sight which is equivalent to the product of elemental transmittance out to a given range.

Radiant heat flux for house 40 is shown in Figure 14. The maximum RHF along the profile of 8.7 kW/m^2 occurs near the edge of the unmanaged fuel at 27m from the house. The integrated energy along the RHF profile indicates a total accumulated energy exposure of nearly 2000J.

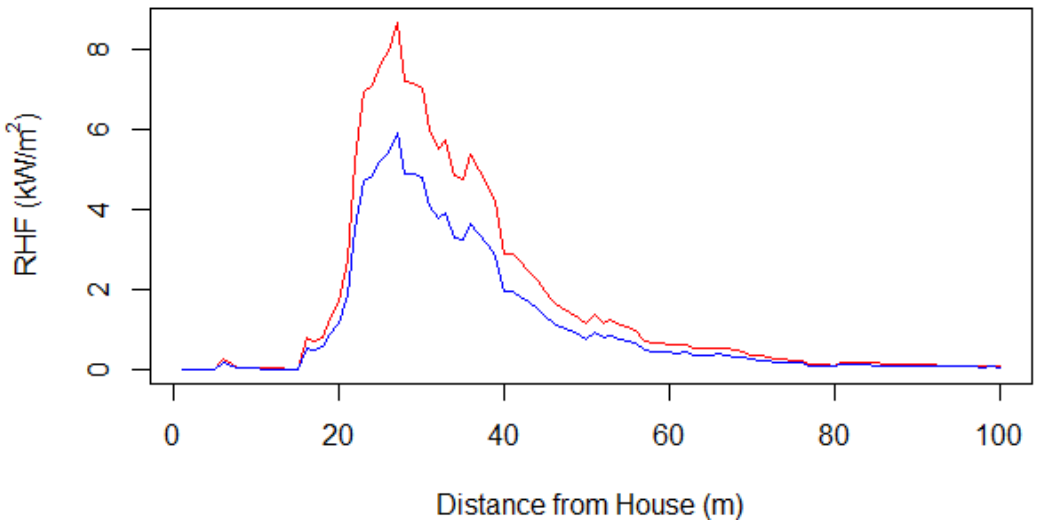

Figure 14: Radiant heat flux profile for house 40 (in red with flame temperature of 1200K and in blue with flame temperature of 1090K).

HOUSE 552

House with survey reference 552 is located approximately 30m west of Buena Vista Road within bushland and had no obvious fuel management. Although the house sustained some damage it was not destroyed by the fire. The fire approach direction was from bushland in the opposite direction from the road.

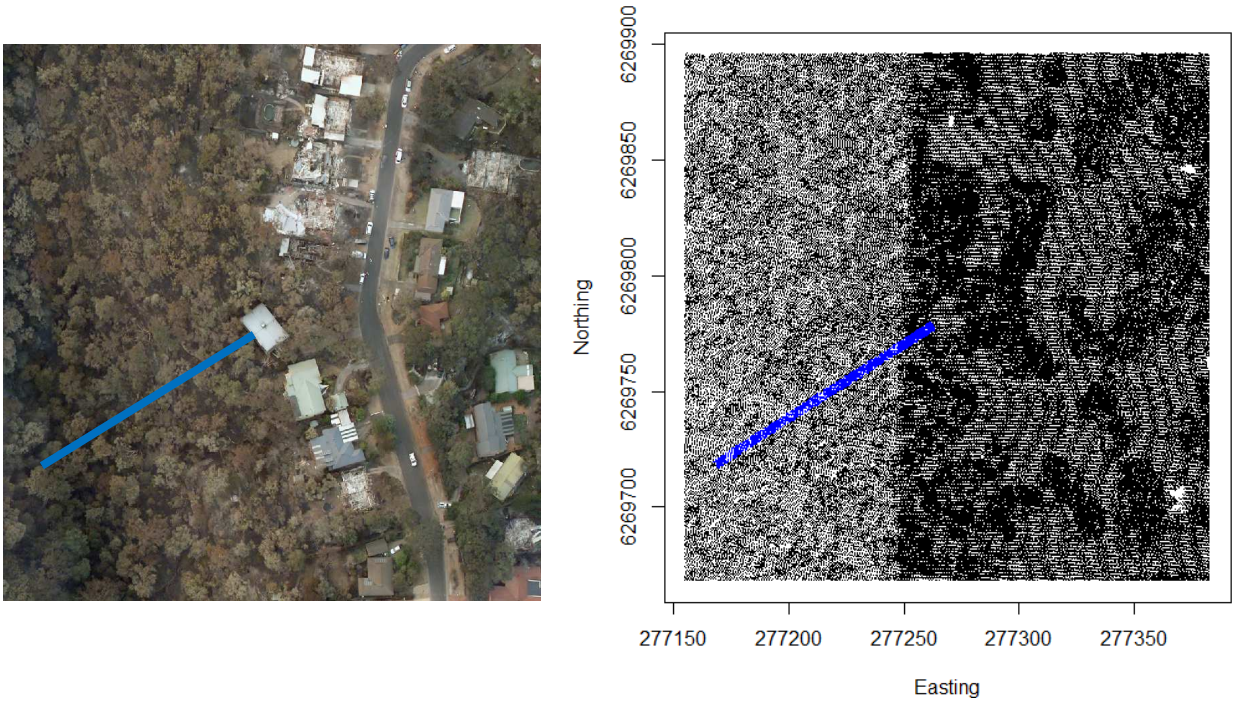

Figure 15: House 552 is within bushland, with no obvious fuel management in the surrounding area. The house is located at the centre of each image in (left) true colour aerial imagery and (right) the lidar point cloud shown from above with the fire approach direction shown in blue.

Lidar points extracted along the transect from the house in the fire approach direction (Figure 16) indicate a consistent forest fuel structure with tree height around 20m. The density of the vegetation (projected cover and LAI) is shown to increase in the 15m closest to the house. The lidar points show the form of the upper canopy very clearly. Beneath the overstorey, areas where no lidar returns are shown may misrepresent the true density of vegetation in these lower strata. The structure of trunks and loose bark fuels, which have a low vertical projected area to mass ratio, are likely not captured accurately by the lidar data because of their low vertically projected area to volume ratio. These vertical elements of the vegetation have been described as erectophile (Ross, 1981) and given our assumption of random projection, may lead to an underestimation of fuel load and the attenuation in the mid-storey.

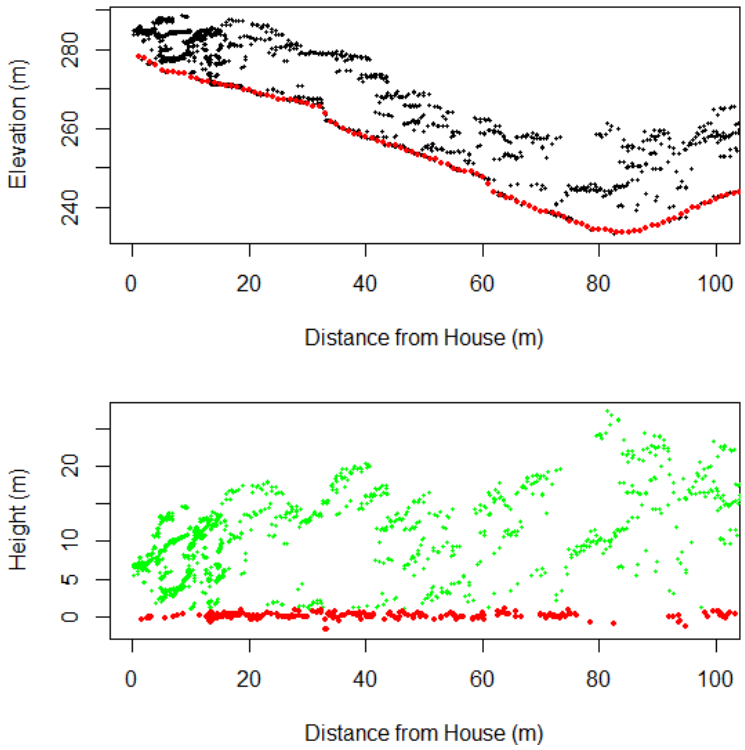

Figure 16: Lidar points extracted along the transect from house 552 in the fire approach direction: (top) the elevation of lidar points are shown in black above the raster DEM in red; (bottom) shows lidar points classified as ground (red) or vegetation (green). Height on the y-axis is height above the terrain surface.

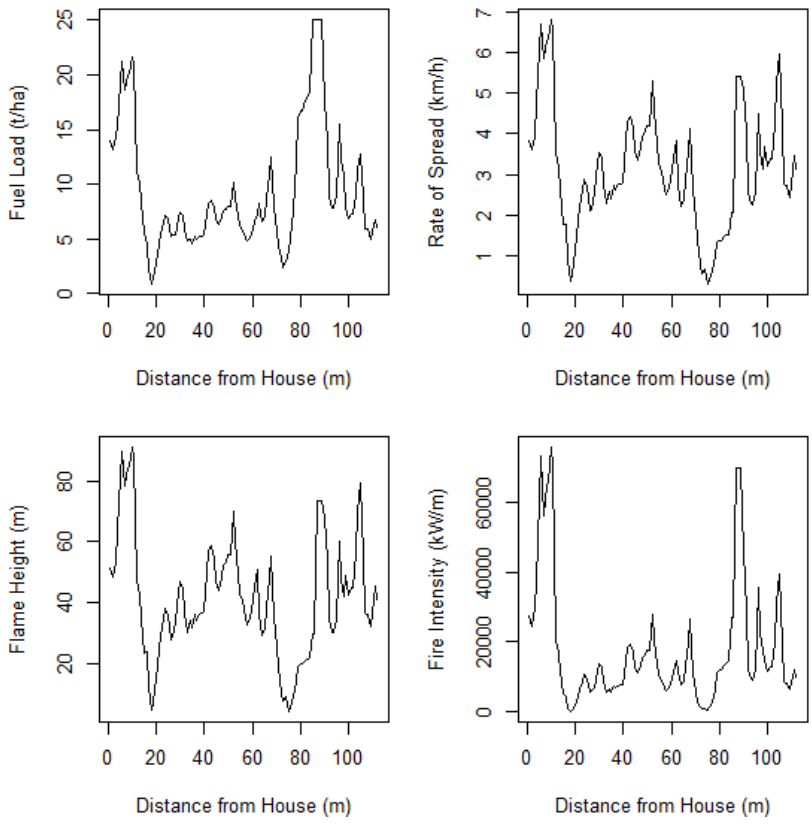

Figure 17: Transects in the fire approach direction from house 552 showing the (top left) fuel load, (top right) slope corrected fire rate of spread, (bottom left) modelled flame height and (bottom right) fire line intensity.

Estimated fuel loads adjacent to house 552 are much higher than for house 40. Even in the areas of bushland outside the managed zone around house 40, fuel loads are shown to peak at 8 t/ha, while for house 552 the fuel load exceeds 20 t/ha at points along the transect (Figure 17). Again the distribution of fuel loads along the transect is the controlling factor in the modelled fire behaviour, along with topographic variation which limits the rate of spread and flame height between 80 and 100m due to a downward progression of the fire.

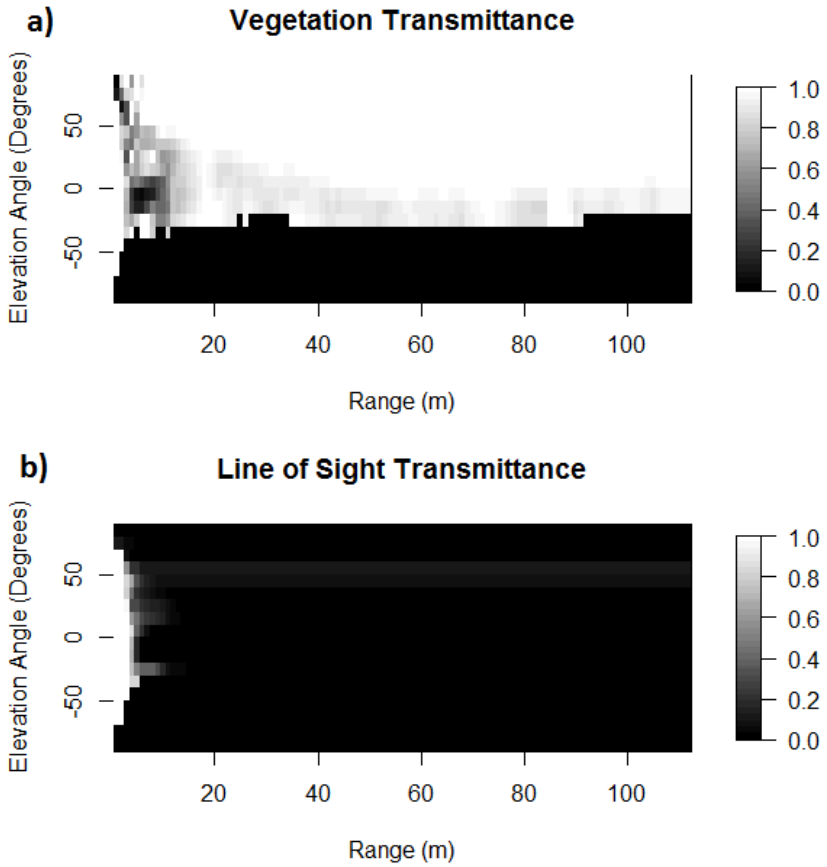

Figure 18: Transmittance out to 100m along lines of sight at different elevation angles from 90 degrees below the horizon to 90 degrees above the horizon: a) the transmittance for each elemental region within the canopy, b) the cumulative transmittance out to a given range along the lines of sight (product of elemental transmittance values).

The effect of dense vegetation near the house can be seen in the transmittance in Figure 18. This blocks most of the radiant heat until the fire front is around 10m from the house. When no attenuation is considered, the AS3959 view factor increases exponentially as the flame front approaches the house. Incorporating attenuation has the effect of increasing the power of this exponential increase such that the RHF close to the house rises from benign to extreme in the final metres. This increase is shown in Figure 19 where modelled RHF is 2.9kW/m^2 when the flame front is 20m from the house, increasing to 8.4kW/m^2 at 10m and to 52.5 kW/m^2 at a range of 2m.

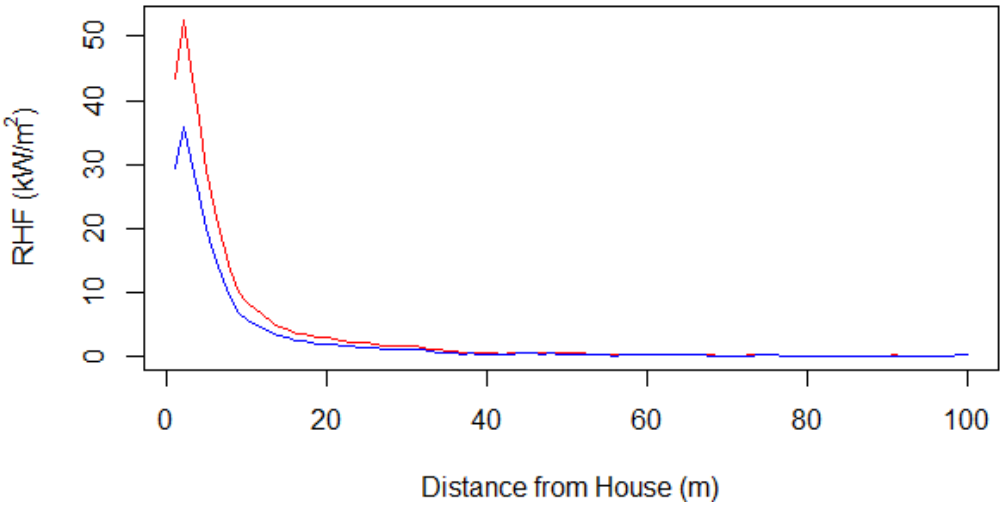

Figure 19: Radiant heat flux profile for house 552 (in red with flame temperature of 1200K and in blue with flame temperature of 1090K).

5.3 Modelled Radiant Heat Flux

The first results of RHF are presented with a flame of 1200K (Table 6, Figure 20 and Figure 21). In most cases the homes within the study area backed onto bushland. The increased level of exposure due to this bushland is illustrated by the steep (exponential) increase in RHF at close range to homes in Figure 20. The Bushfire Attack Level (BAL) as defined in AS3959 is an estimate of the peak radiation exposure received at the house. The calculation of BAL is based on the Fire Danger Index, the slope of the land and the types of surrounding vegetation. Six levels of BAL have been defined in AS3959 (Standards Australia, 2009): BAL Low presents no risk, BAL 12.5 under 12.5 KW/m^2 exposure, BAL 19 under 19 KW/m^2 exposure, BAL 29 under 29 KW/m^2 exposure, BAL 40 under 40 KW/m^2 exposure, BAL FZ presents direct exposure to flame.

A total of 29 homes exceeded the AS3959 BAL 40 threshold, while 79 exceeded BAL 29. The model indicated that only 36 houses were below BAL 12.5.

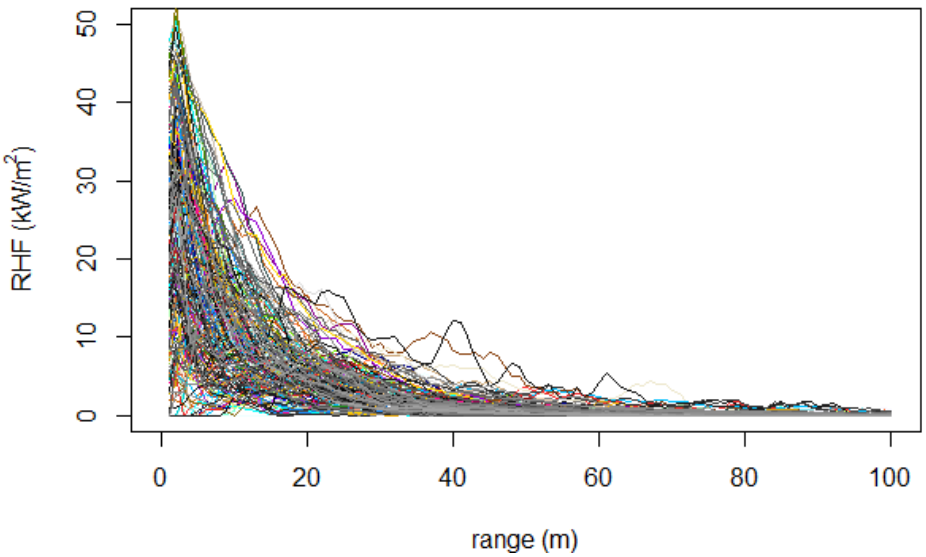

Figure 20: Summary of all 216 radiant heat flux profiles for the homes in the Springwood case study area (with flame temperature 1200K).

No significant separability was shown to exist between the metrics describing the level of RHF exposure for damaged and untouched homes (Table 6 and Figure 21). Of the metrics tested, the maximum RHF and the duration of exposure to greater than 12kW/m^2 provided the greatest separability (Table 6) although only at the 75% confidence level.

Table 6: Summary statistics for the RHF exposure profiles for damaged and untouched homes, along with the probability of separability using a t-test (flame temperature 1200K).

	mean damaged	mean untouched	median damaged	median untouched	p-value
Time100m (s)	464.81	480.71	418.71	405.38	0.67
RHFmax (KW/m^2)	26.09	24.07	26.68	21.32	0.23
E (J)	1956.48	1705.55	1263.69	1115.35	0.33
Tgt12 (s)	54.56	41.73	27.98	18.97	0.23

Given the conditions on the day of the fire the modelled RHF profiles were high. However the estimated time taken for the fire to travel the last 100m before impacting houses was significantly higher than expected given high RHF levels, ranging from 88 seconds to around 30 minutes (Figure 21). Tran et al. (1992) suggested that exposure to RHF levels greater than 12 kW/m^2 for longer than 30 seconds is enough to ignite timber housing materials. The model indicated that 96 homes (44%) were subjected to 12 kW/m^2 exposure for greater than 30 seconds (Figure 21). However, of these homes, 52 were damaged while 44 were untouched.

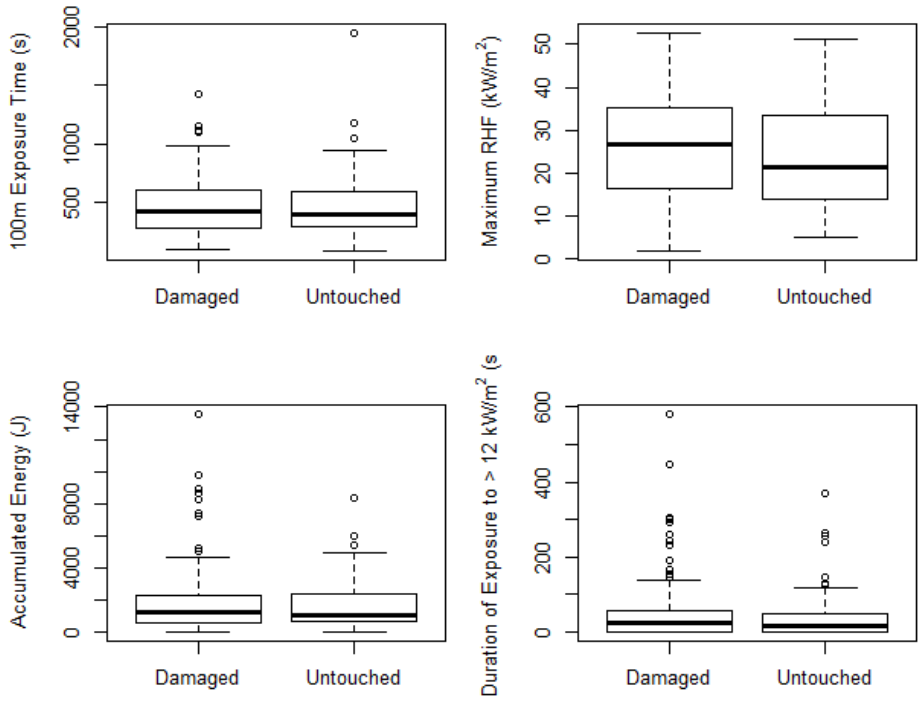

Figure 21: Distribution of RHF metrics for damaged and untouched homes using a flame temperature of 1200K.

Using an assumed flame temperature of 1090K resulted in a predictable reduction in the RHF profiles for each house (Figure 22). Peak RHF for all houses is reduced from 52.5 kW/m^2 to 35.8 kW/m^2, representing a reduction of 32% in maximum RHF. A t-test for separability between RHF metrics for damaged and untouched homes again showed low significance levels except for time of exposure to greater than 12kW/m^2, which is significant at the 95% confidence level (Table 7). This is due primarily to the increase in the increased number of untouched houses that were modelled as having zero exposure to greater than 12kW/m^2 using the 1090K flame temperature.

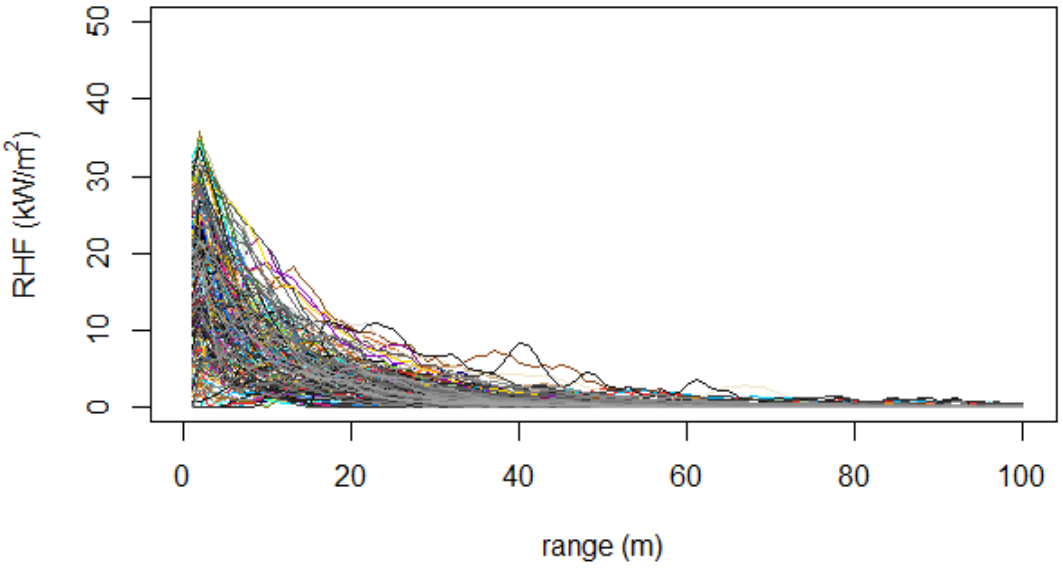

Figure 22: Summary of all 216 radiant heat flux profiles for the homes in the Springwood case study area (with flame temperature 1090K).

Table 7: Summary statistics for the RHF exposure profiles for damaged and untouched homes, along with the probability of separability using a t-test (flame temperature 1090K).

	mean damaged	mean untouched	median damaged	median untouched	p-value
Time100m (s)	464.81	480.71	418.71	405.38	0.67
RHFmax (KW/m^2)	17.76	16.38	18.16	14.51	0.23
E (J)	1331.85	1161.03	860.24	759.26	0.33
Tgt12 (s)	34.05	19.21	10.85	0.00	0.04

The distribution of RHF metrics shown in Figure 23 for 1090K is similar to those shown in Figure 21 for 1200K. As the rate of spread described in the methods section is not temperature dependent, the time taken for the fire to travel the last 100m is the same in both figures. However, negative shifts are shown in the maximum RHF, accumulated energy and the duration of exposure to greater than 12kW/m^2.

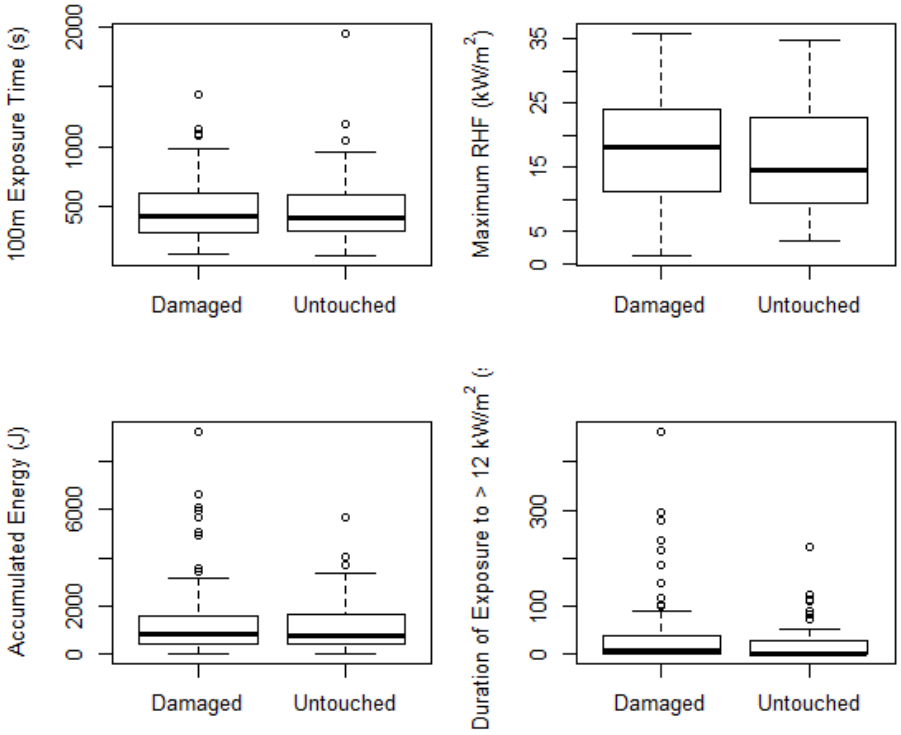

Figure 23: Distribution of RHF metrics for damaged and untouched homes using a flame temperature of 1090K.

6 Discussion

Airborne lidar provides detailed vegetation structural information that is unparalleled for landscape level analyses of fire fuel structure. In our initial case study, Siggins et al. (2013) presented a full three-dimensional ray tracing approach for modelling RHF incident on homes during a bushfire. This model used vegetation structure derived from airborne lidar data to build the three-dimensional simulation environment in which modelling was performed. In this case, vegetation within the scene was represented by opaque spherical crowns whose size was modified to correspond to the density of lidar points in the region.

Given that airborne lidar data is not always available for the time and location required for fire hazard assessment, case study 2 targeted the development of a more generic approach to modelling. The case study utilised low resolution datasets that are available at the continental scale, such that the same modelling could be applied at any location within Australia (Newnham et al., 2013). The modelling approach maintained the consideration of spatially variable fuel loads (although at a coarser scale) and the attenuation of RHF by topographic shadowing and vegetation between the fire front and the house.

This case study reinvestigates the use of the full three-dimensional ray tracing approach using airborne lidar. Rather than modelling vegetation as opaque spheroidal crowns as in case study 1, this case study has represented vegetation using the turbid medium approach where partial attenuation is determined by lidar point density. The effect of other buildings in the vicinity of the house under investigation has also been included as a possible source of radiant heat attenuation. The process for estimation of the view factor, and hence RHF, is essentially ray tracing. However the ray may reach the house with some fraction of its original radiative capacity rather than a binary interception of transmission as in case study 1.

The two individual house RHF exposure profile examples demonstrate how local vegetation and topography are integrated within the modelling framework. The benefit of modelling fire progression across the landscape in the vicinity of a house is that this allows the generation of time based radiation profiles and analysis of time related metrics related to thresholds for building material ignition. The two profiles demonstrate that radiation only became significant as the flames moved into the last 20m of vegetation and peaked as the flame front emerged for it. The modelling approach does not prescribe particular planting or clearing regimes but provides the ability to model the effect of proposed vegetation management strategies. The time radiation profiles also demonstrate the relative difference of 32% in peak radiation exposure when moving from an assumed flame temperature of 1200K to 1090K.

An unusual aspect of this case study is the moderate fire weather severity (FFDI 55) on the day of the fire. Observations during the post-fire survey indicated that canopy fuels played little part in the fire and that generally fire intensities were low relative to previous fires studies (case studies 1 and 2). This resulted in a low prevalence of observed radiation (4%) and flame contact (3%) as the primary mechanism for house damage. Hence, ember related ignition may be a more significant predictor of house damage in this case. This is shown in the correlation between the prevalence of overhanging trees and the damage state of the house in Table 5. Overhanging trees emphasise how leaf deposition plays a significant role in increasing houses vulnerability to ember ignition, rather than the overhanging trees themselves acting as a direct source of radiant heat and flame contact.

The comparison of RHF exposure metrics and house damage provided a low statistically significant correlation except in the case of the time spent above which radiation exceeded 12kW/m^2, specifically when a flame temperature of 1090K was applied. While this was the most significant indicator of damage, prediction provided relatively less confidence compared to the previous two case studies. This emphasises the fact that the RHF metrics did not perform well as a surrogate for overall exposure (including the hazard associated with embers).

7 Conclusion

The RHF modelling presented in this report is the last in a series of three case studies being used to test assumptions regarding the links between RHF exposure and site based assessments of bushfire hazard. The objective of the modelling studies performed is twofold:

1. allow investigation of complex spatial processes (effects on rate of spread, attenuation of RHF by topography and vegetation, etc.) that may impact RHF profiles incident on a house;
2. develop potential methods for assessments of hazard for informing decisions on site preparation and house construction which might assist in developing risk mitigation strategies.

Of the RHF exposure metrics assessed in this study the time in which the radiation exceeded 12kW/m^2 for a flame temperature of 1090K provided the highest confidence in predicting house damage. This indicated that 96 homes (44%) were subjected to 12 kW/m^2 exposure for greater than 30 seconds. However, the modelled results were not statistically significant in explaining house damage as in previous case studies.

Forest fuel loads, including the level of surface fuels and the proximity to houses was relatively consistent across the study area. It is assumed that this lack of fuel management had some influence on the level of risk posed by the Springwood fire. The lack of variability in fuel structure and the importance of embers (as opposed to radiant heat) was one factor in the lack of significance of RHF metrics in explaining house damage. In fact the prevalence of overhanging trees and level of maintenance of the accumulating fuels that occurred near homes from these overhanging trees was shown to explain a greater proportion of the probability of house loss in this case study.

8 References

Asner, G. (2003). Global synthesis of leaf area index observations: implications for ecological and remote sensing studies. *Global Ecology and …*. [Online]. Available from: http://onlinelibrary.wiley.com/doi/10.1046/j.1466-822X.2003.00026.x/full. [Accessed: 20 May 2014].

Blanchi, R., Leonard, J., Culvenor, D., Newnham, G., Opie, K. & Siggins, A. (2011). *Vulnerability Model Parameters: Literature Review*. Melbourne: CSIRO Ecosystems Sciences - Land and Water - Bushfire CRC report.

BOM (2013a). *Monthly Weather Review Australia, October 2013*. [Online]. Melbourne. Available from: http://www.bom.gov.au/climate/mwr/aus/mwr-aus-201310.pdf.

BOM (2013b). *Monthly Weather Review Australia, September 2013*. [Online]. Melbourne. Available from: http://www.bom.gov.au/climate/mwr/aus/mwr-aus-201309.pdf.

Byram, G.M. (1959). Combustian of Fuels. In: K. P. Davis (ed.). *Forest Fire Control and Use*. McGraw-Hill, pp. 61–89.

Leonard, J. & Blanchi, R. (2005). Report for ACT Coroner. Formerly Confidential Document CMIT(C)-2005-377 but advised 8-12-05 no longer confidential. $$AR/N/R. *Investigation of bushfire attack mechanisms involved in house loss in the ACT Bushfire 2003*. CSIRO Manufacturing & Infrastructure Technology.

Leonard, J., Blanchi, R., Leicester, R., Lipkin, F., Newnham, G., Siggins, A., Opie, K., Culvenor, B., Cechet, B., Corby, N., Thomas, C., Habili, N., Jakab, M., Coghlan, R., Lorenzin, G., Campbell, D. & Barwick, M. (2009). *Building and Land use planning research after the 7th February 2009 Victorian bushfires. Preliminary findings*. [Online]. Melbourne: Interim report USP2008/018 - CAF122-2-12 . Available from: http://www.bushfirecrc.com/managed/resource/bushfire-crc-victorian-fires-research-taskforce-final-report.pdf.

Leonard, J., Blanchi, R., Newnham, G., Culvenor, D., Siggins, A. & Opie, K. (2011). *Characterisation of interface fuels–literature review, Bushfire CRC report*.

Leonard, J., Blanchi, R., Newnham, G., Siggins, A., Opie, K., Lipkin, F. & Culvenor, D. (2012). *Work Program Objectives and Approach – Identifying neighbourhood scale parameters*. Melbourne: CSIRO Ecosystems Sciences - Land and Water - Bushfire CRC report.

Luke, R. & McArthur, A. (1978). *Bush fires in Australia.* Reprinted . Canberra Publishing and Printing Co.

McArthur, A.G. (1973). *Forest Fire Danger Meter Mark V*. [Online]. Available from: Forestry Research Institute, Forestry and Timber.

McArthur, A.G. (1967). *Grassland Fire Danger Meter Mk IV*. [Online]. Available from: Bush Fire Council of N.S.W. Officer Training Module CL/4 - Fire Behaviour Second Edition.

Newnham, G., Blanchi, R., Siggins, A., Opie, K. & Leonard, J. (2013). *Bushfire Decision Support Toolbox Radiant Heat Flux Modelling: Case Study Two, Wangary, South Australia*. Report to the Bushfire Cooperative Research Centre.

Noble, I.R., Bary, G.A.V. & Gill, A.M. (1980). McArthers fire danger meters expressed as equations. *Australian Journal of Ecology*. 5. p.pp. 201–203.

Ramsay McArthur, N.A. Dowling, V.P., G.C. (1987). Preliminary results from an examination of house survival in the 16 February 1983 bushfires in Australia. *Fire and Materials*. 11. p.pp. 49–51.

Ross, I. (1981). *The radiation regime and architecture of plant stands*. [Online]. Available from: http://books.google.com.au/books?hl=en&lr=&id=w6SogqDOa54C&oi=fnd&pg=PR5&dq=radiation+re

gime+and+architecture+of+plant+stands&ots=Z_f8BOg9BT&sig=MiRc9O36pEoFPBcJ6994-9rV8bk. [Accessed: 26 February 2014].

Siggins, A., Leonard, J., Newnham, G., Blanchi, R., Lipkin, F., Opie, K. & Culvenor, D. (2013). *Modelling Radiant Heat Exposure at the Urban Fringe - Pine Ridge Road, Kinglake West, Case Study*.

Standards Australia (2009). *AS 3959-2009 (Amend. 1). Construction of buildings in bushfire-prone areas*. Sydney.

Sullivan, A.L., Ellis, P.F. & Knight, I.K. (2003). A review of radiant heat flux models used in bushfire applications. *International Journal of Wildland Fire*. [Online]. 12 (1). p.p. 101. Available from: http://www.publish.csiro.au/view/journals/dsp_journal_fulltext.cfm?nid=114&f=WF02052. [Accessed: 4 December 2013].

Tran, H.C., Cohen, J.D. & Chase, R.A. (1992). Modeling ignition of structures in wildland/urban interface fires. In: *Proc 1st international fire and materials conference, Arlington, VA*. 1992, pp. 253–262.

Viegas, D.X. & Simeoni, A. (2011). Eruptive Behaviour of Forest Fires. *Fire Technology*. 47 p.pp. 303–320.

Walker, J. (1981). Fuel dynamics in Australian vegetation. *Fire and the Australian biota*.

Wilson, A.A.G., National Centre for Rural Fire Research (Australia) & Chisholm Institute of Technology. (1984). by Andrew A.G. Wilson. 25 cm. *Assessing the bushfire hazard of houses : a quantitative approach*. Melbourne: National Centre for Rural Fire Research, Chisholm Institute of Technology.

Zárate, L., Arnaldos, J. & Casal, J. (2008). Establishing safety distances for wildland fires. *Fire Safety Journal*. 43 (8). p.pp. 565–575.